Interaction between Plasmonic Nanoparticles Revisited with Transformation Optics

Alexandre Aubry, Dang Yuan Lei, Stefan A. Maier, and J. B. Pendry

The Blackett Laboratory, Department of Physics, Imperial College London, London SW72AZ, United Kingdom

The interaction between plasmonic nanoparticles is investigated by means of transformation optics. The optical response of a dimer can be decomposed as a sum of modes whose resonances redshift when the nanoparticles approach each other. The extinction and scattering cross sections as well as the field enhancement induced by the dimer are derived analytically taking into account radiation damping. Interestingly, some invisibility dips occur in the scattering spectrum and originate from a destructive interference between each surface plasmon mode.

The interaction between metallic nanoparticles has attracted a wide range of interest for the past ten years. The physics of this interaction is rich and opens nice perspectives for applications, such as single molecule detection [1,2], solar cells [3], or high harmonic generation [4]. In a dimer of metallic nanoparticles, the localized surface plasmons (LSPs) supported by each monomer can interact between each other: several resonances may arise in the visible or near-infrared spectra [5] and lead to a drastic field enhancement in the narrow gap separating the two nanoparticles [6]. An elegant physical picture to describe this interaction is the plasmon hybridization model [7]. In analogy with molecular orbital theory, the dimer plasmons can be viewed as bonding and antibonding combinations of the individual nanoparticle plasmons. However, albeit elegant, the plasmon hybridization picture is a limited tool: numerical simulations are still needed to calculate the optical response of a dimer.

Recently, an original approach based on transformation optics has been proposed to derive analytically the optical response of complex nanostructures [8]. It consists in finding a conformal map that transforms the plasmonic nanostructure under investigation into a simpler plasmonic system that can be solved analytically. In this Letter, this strategy is applied to investigate the interaction between plasmonic nanoparticles by considering the example of a nanowire dimer. Note that conformal mapping has also been used in the past to study the interaction between dielectric nanoparticles [9] in the context of effective medium theory [10]. The dimer problem can be solved by mapping it onto a system consisting of an array of dipoles sandwiched between two semi-infinite metal slabs (see Fig. 1). The electric field can be decomposed as a sum of modes denoted by a discrete angular momentum n, in agreement with the hybridization picture. Each mode may give rise to a resonance which is redshifted when the two nanowires approach each other. The extinction and scattering cross sections as well as the field enhancement induced in the near-field of the dimer are expressed analytically taking into account radiation damping. Interestingly,

the scattering spectrum displays some *invisibility* dips resulting from the destructive interference between the modes supported by the dimer. At such frequencies, the dimer can harvest light efficiently and focus its energy at the nanoscale without any far-field scattering. This feature can be a promising alternative to the concept of sensor cloaking [11]: a dimer can receive and transmit information to a molecule placed in its near field, while its presence cannot be detected in the far field.

Our original system is an array of line dipoles oriented along the x axis and aligned along the y axis, with pitch 2π, located in a thin slab of insulator of thickness d surrounded by two semi-infinite slabs of plasmonic material for $x < -d/2$ and $x > d/2$ [Fig. 1(a)]. Now we apply the following conformal transformation,
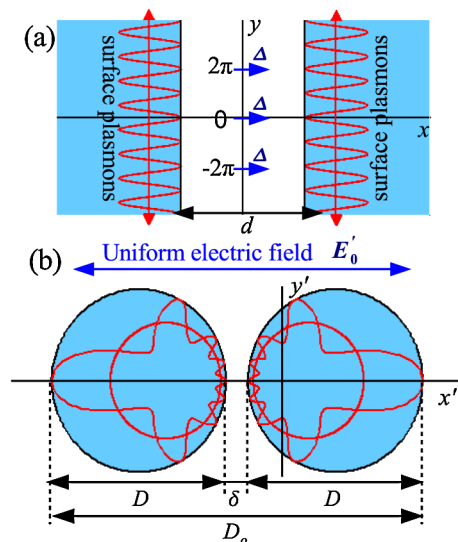
FIG. 1 (color online).   (a) Two semi-infinite metallic slabs separated by a thin dielectric film support SPs that couple to an array of dipoles $\mathbf{\Delta}$ (blue arrows). The array pitch is 2π. (b) The transformed material of (a) is a pair of cylinders of diameter D, separated by a narrow gap δ. The dipole sources $\mathbf{\Delta}$ are transformed into a uniform electric field $\mathbf{E}_0'$.

$$z' = g/[\exp(z) - 1], \qquad (1)$$

$z = x + iy$ and $z' = x' + iy'$ are the usual complex number notations in the original and transformed frames, respectively. g is an arbitrary constant. The transformed material is a dimer of nanowires of diameter $D = g/\sinh(d/2)$ separated by a gap $\delta = g\tanh(d/4)$ [see Fig. 1(b)]. The ratio $\rho = \delta/(2D)$ will be a key parameter in the following.

The transformation of the sources is also shown in Fig. 1. The original dipoles $\mathbf{\Delta}$ are transformed into a uniform electric field $\mathbf{E}_0' = (2\pi\epsilon_0 g)^{-1}\mathbf{\Delta}$. Note that we made the choice of an electric field $\mathbf{E}_0'$ polarized along x' since $\mathbf{\Delta}$ is assumed to be aligned along x. Actually, this polarization is by far more efficient to excite surface plasmon (SP) modes than a polarization along y' [8]. Note also that in the literature, most of the experimental work dealing with metallic nanowires considers SPs propagating along the nanowire axis [12,13] and not in the transverse plane. We shall assume that the dimensions of the cylinder pair are sufficiently small that the SP modes are well described in the near-field approximation. The uniform electric field $\mathbf{E}_0'$ can then be considered as due to an incident plane wave. Furthermore, in this case, the dielectric properties of the nanostructure are the same as those of the slab from which it is derived. Also preserved under the transformation is the electrostatic potential.

The mathematics of the conformal transformation closely links the physics at work in each of the very different geometries. In Fig. 1(a), the array of dipoles pumps energy into the SP modes supported by two semi-infinite metallic slabs. This implies a discrete modal structure for this system: only integer spatial frequencies n can be excited among the overall k spectrum. The same modes are excited by the incident field $\mathbf{E}_0'$ in the transformed geometry [Fig. 1(b)]: only LSP modes displaying an integer number n of spatial periods when propagating around each nanowire can be excited. The transformation shown in Fig. 1 tells us that these modes couple to each other in the narrow gap separating the two nanoparticles: their wavelength and velocity decrease, leading to an important field enhancement at this location. However, contrary to the kissing cylinders [8], their velocity does not vanish; hence, the LSPs turn infinitely around the nanoparticles before being absorbed. This explains their resonant behavior. After this brief qualitative account, we now present the results of our analytical theory.

As shown in a previous study [8], the extinction cross section σ_{ext} of the cylinder pair can be deduced in the quasistatic limit from the power absorbed by each dipole in the original frame. Moreover, radiation damping in the transformed geometry [Fig. 1(b)] can be represented by a fictive absorbing particle in the original frame [14]. It yields the following expression for σ_{ext}:

$$\sigma_{\text{ext}} = \text{Im}\left\{\frac{16\pi k_0 \rho(\rho+1)D^2\beta}{1 - i2\pi\rho(1+\rho)D^2 k_o^2\beta}\right\}, \qquad (2)$$

with

$$\beta = \frac{\epsilon - 1}{\epsilon + 1}\sum_{n=1}^{+\infty}\frac{n}{(\sqrt{\rho}+\sqrt{1+\rho})^{4n} - (\epsilon-1)/(\epsilon+1)}, \qquad (3)$$

$k_0 = \omega/c_0$ is the wave number in vacuum. The effect of radiation damping appears in the denominator of Eq. (2). In the quasistatic limit ($D_0 < 20$ nm), radiation damping is negligible and σ_{ext} is strictly equal to the absorption cross section. The parameter β in Eq. (3) displays the sum of each contribution due to the LSP modes supported by the cylinder pair and denoted by their angular moment n. Each mode may give rise to a resonance at a frequency satisfying the following relation:

$$(\sqrt{\rho}+\sqrt{1+\rho})^{4n} = \text{Re}\{(\epsilon-1)/(\epsilon+1)\}. \qquad (4)$$

Note that this condition of resonance only depends on the ratio $\rho = \delta/(2D)$.

Figure 2 illustrates this resonant feature by displaying σ_{ext}/D_0 as a function of frequency and $\rho = \delta/2D$, for an overall physical cross section $D_0 = 20$ nm. For this figure as well as in the following of the study, the metal is assumed to be silver with a surface plasma frequency $\omega_{\text{SP}} = 3.67$ eV and permittivity taken from Johnson and Christy [15]. As shown by Fig. 2, the absorption spectrum is strongly dependent on ρ and shows three distinct regimes.

(i) Weak coupling regime ($\rho > 0.5$, i.e., for a gap larger than the cylinder diameter).—All the modes resonate at the vicinity of the surface plasma frequency ω_{SP}. The coupling between the two nanoparticles is weak and the system exhibits the same absorption spectrum as an individual cylinder.

(ii) Strong coupling regime ($\rho < 0.5$).—When the two nanoparticles are approached by less than one diameter, resonances for small n start to arise at a smaller frequency than ω_{SP}. These resonances are redshifted when the gap decreases and the absorption spectrum displays several resonances in the visible spectrum in addition to the individual LSPs resonance at ω_{SP}.
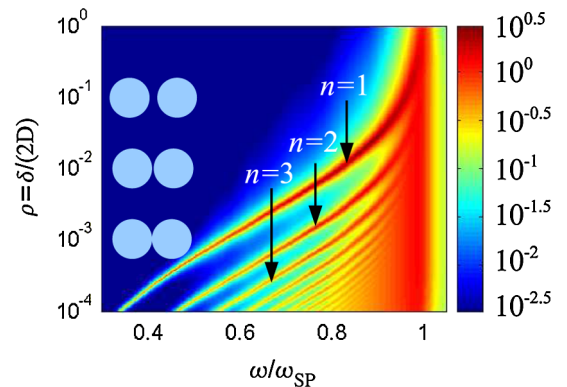
FIG. 2 (color online). Absorption cross section σ_{ext} normalized by the physical cross section D_0 as a function of ρ and frequency for a cylinder pair with $D_0 = 20$ nm. The color bar is in log scale.

(iii) Kissing cylinders regime ($\rho \to 0$).—The number of excited modes becomes infinite, leading to a continuous and broadband absorption spectrum [8].

Note that, in practice, the cylinders can be so close to each other in the strong coupling regime that they would stick by van der Waals attraction. To circumvent that problem, they can be embedded into a dielectric matrix. Our analytic model is still valid in this case except that the term $(\epsilon - 1)/(\epsilon + 1)$ should be replaced by $(\epsilon - \epsilon_d)/(\epsilon + \epsilon_d)$ in Eq. (3) (with ϵ_d the permittivity of the dielectric matrix).

Figure 3(a) shows the effect of radiative damping on the extinction spectrum for different sizes of dimers at a fixed ratio $\rho = 0.01$. The theoretical predictions [Eq. (2)] are compared to the results of numerical simulations performed with the software COMSOL. An excellent agreement is found in the quasistatic limit ($D_0 = 20$ nm). For larger structure dimensions, the numerical results are slightly redshifted compared to our theoretical predictions. This is due to the retardation effects which are not considered by our approach [14]. However, the magnitude and line shape of resonances are nicely predicted for structure dimension up to 200 nm. Figure 3(a) shows that radiative damping broadens the linewidth of each resonance and leads to the saturation of the extinction cross section at the level of the physical cross section.

An expression of the scattering cross section σ_s can also be derived following the strategy of Ref. [14]:

(a)

(b)

FIG. 3 (color online).   Extinction cross section σ_{ext} (a) and scattering cross section σ_s (b), normalized by the physical cross section D_0, plotted as a function of frequency for nanowire dimers of different sizes with $\rho = 0.01$. The theoretical predictions (continuous lines) are compared to the results of numerical simulations (dots).

$$\sigma_s = \frac{32\pi^2 k_o^3 \rho^2 (1 + \rho)^2 D^4 |\beta|^2}{|1 - i2\pi\rho(1 + \rho)D^2 k_o^2 \beta|^2}. \quad (5)$$

The radiative spectrum depends on $|\beta|^2$ [Eq. (3)]. Hence, the resonances defined by Eq. (4) also occur in the scattering spectrum [Eq. (4)]. This is confirmed by Fig. 3(b) which displays σ_s/D_0 as a function of frequency for different sizes of dimers at a fixed ratio $\rho = 0.01$. There is a perfect agreement between our theoretical prediction and the numerical result in the quasistatic limit ($D_0 = 20$ nm). The resonances displayed by Fig. 3(b) clearly display an asymmetric line shape. We stress the fact that these are not Fano resonances which appear usually in the extinction spectrum and correspond to the coupling between bright and dark modes. The sharp dips observed in Fig. 3(b) originate from the destructive interference between each successive bright mode. Typically, the sharp dip observed at $\omega = 0.85\omega_{\text{SP}}$ results from the destructive interference between the modes $n = 1$ and $n = 2$ which resonate on each side of the dip. This feature can be promising in the perspective of sensing applications, since the ratio between the absorption and scattering cross sections can reach, for instance, a value of 150 in the conditions considered in Fig. 3(b). At these invisibility frequencies, the nanowire dimer can harvest light efficiently from the far field and focus its energy at the nanoscale, without any scattering toward the surrounding area. The dimer acts then as an invisible or noninvasive sensor.

As for the extinction cross section, radiation damping leads to a renormalization of the scattering cross section for large structure dimensions [see the denominator in Eq. (5)] which makes σ_s saturate at the level of the physical cross section [see Fig. 3(b)]. A satisfying agreement is found between numerical and analytical results in Fig. 3(b), except for the slight redshift explained by retardation effects. The Q factor of the invisibility dips decreases for large structure dimensions, and the nanowire dimer may keep its invisible feature only for dimension inferior to 100 nm.

The electric field $\mathbf{E}'(x', y')$ induced by the dimer can be deduced from the electrostatic potential solved in the original frame [Fig. 1(a)]. It can be decomposed as an infinite sum of modes $\mathbf{\Psi}^{(\mathbf{n})}$: $\mathbf{E}' = \sum_{n=1}^{\infty} \mathbf{\Psi}^{(\mathbf{n})}$. Their expression along the y' direction outside of the nanowire dimer is the following:

$$\psi_{y'}^{(n)} = 2inE_0'\rho(1+\rho)D^2\left[\frac{\epsilon+1}{\epsilon-1}(\sqrt{\rho}+\sqrt{1+\rho})^{4n}-1\right]^{-1}$$
$$\times \{[u^{n-1}+u^{-n-1}]/z'^2 - [(u^*)^{n-1}+(u^*)^{-n-1}]/z'^{*2}\},$$

with $u = 1 + 2\sqrt{\rho(1+\rho)}D/z'$.

Figure 4 shows the result of our analytical calculation of the two first modes taken at their resonant frequencies [Eq. (4)]. The gap δ is fixed to $D/50$ ($\rho = 0.01$). As pointed out previously, each nanowire supports LSPs which couple to each other in the narrow gap, leading to an important field enhancement at this location. The
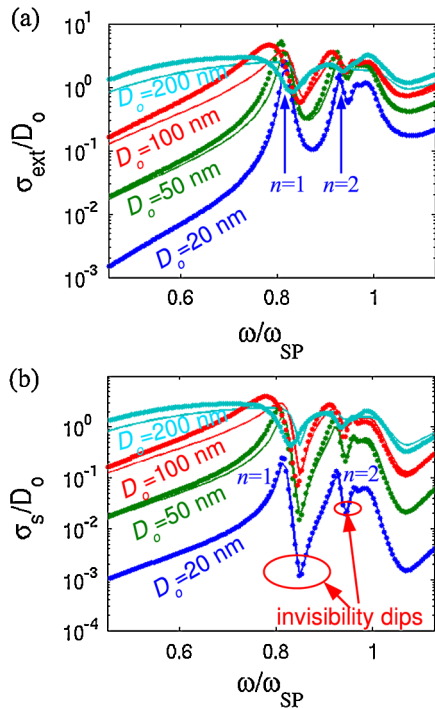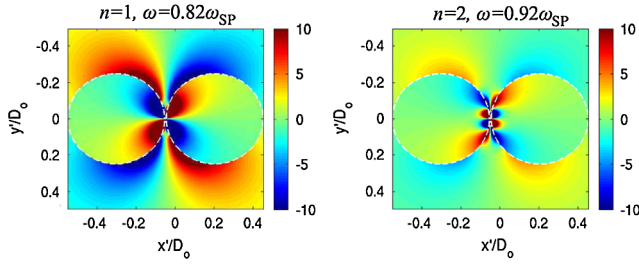
FIG. 4 (color online). Imaginary part of $\psi^{(1)}_{y'}$ (left) and $\psi^{(2)}_{y'}$ (right) normalized by the incoming field E'_0 at their resonant frequencies [Eq. (4)] for $\rho = 0.01$. The color scale is restricted to $[-10 \; 10]$, but note that the field magnitude can be by far larger in the gap.

angular momentum n associated with each mode corresponds to the number of spatial periods covered by the LSPs when they propagate around each nanowire.

Figure 5 shows a more systematic investigation of the nanofocusing properties of a dimer. The field enhancement, $|E'|/E'_0$, observed along the surface of the nanowires is shown as a function of the angle θ (defined in the inset of Fig. 5) and frequency for different values of ρ. Note that the results displayed by Fig. 5 are valid in the quasistatic limit: the field enhancement should be renormalized by a factor $|1 - 2i\pi\rho(1 + \rho)D^2 k_o^2\beta|$ when radiation damping is no longer negligible ($D_0 > 20$ nm). Note also that, for a gap inferior to 0.5 nm between the nanowires, quantum mechanical and nonlocal effects have to be taken into account and may also reduce the field enhancement relative to classical predictions [16].

The resonances of the first LSP modes are clearly visible in Fig. 5. Each resonance leads to a drastic field enhance-

ment that can be superior to 10^3 for $\rho < 0.01$. Figure 5 also shows that the field spreads spatially over a large part of the cylinder surface ($|\theta| < 50°$), contrary to kissing cylinders for which the energy is extremely confined at the vicinity of the touching point [8]. Unlike the scattering spectrum which shows invisibility dips [Fig. 3(b)], a strong field enhancement ($> 10^2$) is still obtained out of resonance: the interference between LSP modes is destructive in the far-field but not in the near field. This invisible feature may be of fundamental interest for applications in biology and nano-optics.

To conclude, note that the conformal transformation approach can be extended to a wide range of nanostructures (crescents, 3D dimers, nanoshells, etc.). More than simply elegant, this strategy is powerful since it provides novel physical insights (e.g., the invisibility dips) and a fully analytical solution to describe the physics of LSPs in complex nanostructures. Unlike a numerical approach, an efficient and rapid optimization of the nanostructures can be performed as a function of the application considered. Further improvements in our analytic model would be to include quantum mechanical and nonlocal effects [16]. An atomistic approach might also be necessary to go beyond the continuum approximation for subnanometer interparticle distance.

FIG. 5 (color online). Field enhancement $|E'|/E'_0$ arising at the surface of the cylinders, plotted as a function of the angle θ and frequency, for different gaps between the two nanoparticles. The color bars are in log scale.

[1] S. Nie and S. R. Emory, Science **275**, 1102 (1997).
[2] K. Kneipp *et al.*, Phys. Rev. Lett. **78**, 1667 (1997).
[3] H. A. Atwater and A. Polman, Nature Mater. **9**, 205 (2010).
[4] S. Kim *et al.*, Nature (London) **453**, 757 (2008).
[5] K.-H. Su *et al.*, Nano Lett. **3**, 1087 (2003); T. Atay, J-H. Song, and V. Nurmikko, Nano Lett. **4**, 1627 (2004); I. Romero *et al.*, Opt. Express **14**, 9988 (2006).
[6] K. Li, M. I. Stockman, and D. J. Bergman, Phys. Rev. Lett. **91**, 227402 (2003); J. P. Kottmann and O. J. F. Martin, Opt. Express **8**, 655 (2001); E. Hao and G. C. Schatz, J. Chem. Phys. **120**, 357 (2004).
[7] P. Nordlander *et al.*, Nano Lett. **4**, 899 (2004).
[8] A. Aubry *et al.*, Nano Lett. **10**, 2574 (2010).
[9] R. C. McPhedran *et al.*, Appl. Phys. **23**, 223 (1980).
[10] D. J. Bergman, Phys. Rev. B **19**, 2359 (1979); J. Phys. C **12**, 4947 (1979).
[11] A. Alú and N. Engheta, Phys. Rev. Lett. **102**, 233901 (2009).
[12] A. V. Akimov, *et al.*, Nature (London) **450**, 402 (2007).
[13] H. W. Lee, *et al.*, Appl. Phys. Lett. **93**, 111102 (2008).
[14] A. Aubry *et al.*, Phys. Rev. B **82**, 205109 (2010).
[15] P. B. Johnson and R. W. Christy, Phys. Rev. B **6**, 4370 (1972).
[16] J. Zuloaga, E. Prodan, and P. Nordlander, Nano Lett. **9**, 887 (2009); J. M. McMahon, S. K. Gray, and G. C. Schatz, Nano Lett. **10**, 3473 (2010).